

Fundamental trade-off between the speed of light and fluctuations in photon current in coherently controlled Lambda systems

Davinder Singh,¹ Seogjoo J. Jang,² and Changbong Hyeon^{1,*}

¹*Korea Institute for Advanced Study, Seoul 02455, Korea*

²*Department of Chemistry and Biochemistry, Queens College,*

City University of New York, 65-30 Kissena Boulevard, Queens, New York 11367, USA and Chemistry and Physics PhD Programs and Initiative for Theoretical Sciences, Graduate Center, City University of New York, 365 Fifth Avenue, New York 10016, USA

Coherently controlled Λ -type three-level atomic systems, which significantly slow down the group velocity of light and can be utilized for building quantum memory devices, feature nonequilibrium current of photon transitions between the three electronic states. We provide a fundamental trade-off between the group velocity of light and the fluctuations in the photon current of Λ -system. Regardless of the atomic type comprising the media, at two-photon resonance condition of control and probe pulses, the Fano factor of the photon current maximizes to 3 at the minimal velocity of light.

Introduction. Since the seminal work by Hau *et al.* [1], which demonstrated extraordinary slowdown of the group velocity of light propagating through an ultracold gas of sodium atoms as low as 17 m/s, there have been considerable efforts to develop an optical quantum memory device to store and retrieve quantum states of light on demand [2–8]. The electronic state of sodium atoms constitute a Λ -type three-level system, which comprises two nearly degenerate ground states and a common excited state. Applying a control pulse to the Λ -system can eliminate the linear absorption of a resonant probe pulse. Depending on the intensity of the control pulse relative to the probe pulse, two distinct mechanisms, coherent population trapping (CPT) [9, 10] and electromagnetically induced transparency (EIT) [11] (see Supplemental Material), transform an otherwise absorbing medium effectively transparent and slow down the group velocity of the probe pulse propagating through the media [6]. While conceptually clear, realization of an actual quantum memory device is often beset with a substantial level of noise [12, 13], and the precise origin of the noise is currently left unknown in many cases. Thus, elucidating the origin and intrinsic limit of such noise level is a crucial step in overcoming practical challenges.

Quantifying the nonequilibrium fluctuations arising from dynamical processes is a fundamental issue [14–16], for which significant advances have been made towards the quantum extension of stochastic thermodynamics [17–22]. Our recent analysis of a coherent field-driven two-level system (TLS) weakly interacting with bosonic environment [22] provides a hint at the above issue concerning the noise in Λ -systems. It has shown that in the field-driven TLS, the fluctuations in photon current are determined by the competition between the real and imaginary parts of the steady state coherence

formed between the excited and ground states, such that the imaginary part of the coherence reduces the fluctuations, whereas the real part contributes to enhancing them [22].

The main objective of this work is to offer quantitative understanding of how the fluctuations in photon current of a coherently controlled Λ -system change when the group velocity of light passing through the associated media is reduced. To this end, we extend the formalism that have been employed for the field-driven TLS to the Λ -system, and clarify the relationship between the group velocity of light across the medium composed of Λ -type three-level atomic systems and fluctuations in photon current. Our study highlights a fundamental trade-off between the speed of light and the fluctuations.

Theoretical model. A three-level Λ -system comprised of the electronic states $|1\rangle$, $|2\rangle$, and $|3\rangle$ is coupled to a thermally-equilibrated bosonic bath at temperature T . The system is illuminated with control ($\alpha = c$) and probe ($\alpha = p$) laser pulses, $\vec{E}_\alpha = \hat{\epsilon}_\alpha \zeta_\alpha (e^{i\omega_\alpha t} + e^{-i\omega_\alpha t})$, each with the amplitude ζ_α , the angular frequency ω_α , and the two polarization vectors satisfying $\hat{\epsilon}_c \cdot \hat{\epsilon}_p = 0$. The atoms in $|2\rangle$ and $|3\rangle$ states are excited to a common excited state $|1\rangle$ through the interactions of transition dipoles, \vec{d}_2 (between $|1\rangle$ and $|2\rangle$) and \vec{d}_3 (between $|1\rangle$ and $|3\rangle$) with the pulses (see Fig. 1A), which are represented by an interaction Hamiltonian $H_{\text{int}} = -\vec{d}_2 \cdot \vec{E}_c - \vec{d}_3 \cdot \vec{E}_p$. These interactions are characterized by corresponding Rabi frequencies Ω_c and Ω_p (see SM for details). Illuminated by the pulses, the atom in the state $|1\rangle$ can either decay into $|2\rangle$ with a rate γ_{12} or into $|3\rangle$ with γ_{13} . The transition between $|2\rangle$ and $|3\rangle$ is effectively spin-disallowed with $\gamma_{23} \ll \gamma_{12}, \gamma_{13}$. With the standard assumptions of the weak system-bath coupling, Born-Markov, and the ro-

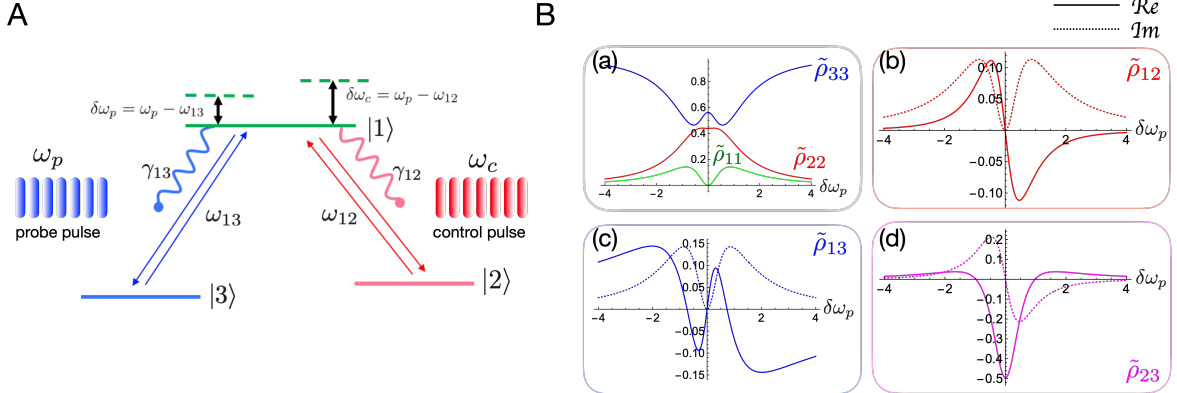


FIG. 1. Optical properties of Λ -system as a function of detuning frequency ($\delta\omega_p$). (A) Schematic of the system consisting of 3 electronic states, $|1\rangle$, $|2\rangle$ and $|3\rangle$, interacting with the probe and control pulses of frequencies ω_p and ω_c . Here, $\omega_{12} (\equiv \omega_1 - \omega_2)$ and $\omega_{13} (\equiv \omega_1 - \omega_3)$ are the resonant frequencies. Further, $\delta\omega_c = \omega_c - \omega_{12}$ and $\delta\omega_p = \omega_p - \omega_{13}$ denote the detuning frequencies. The condition $\delta\omega_p = \delta\omega_c = 0$ corresponds to the two-photon resonance. (B) Populations in $|1\rangle$, $|2\rangle$, and $|3\rangle$ are shown in the panel (a). Real and imaginary parts of the coherences $\tilde{\rho}_{12}$, $\tilde{\rho}_{13}$, and $\tilde{\rho}_{23}$ are depicted in (b), (c), and (d) as a function of $\delta\omega_p$ with the solid and dotted lines, respectively. Here, we have used $\gamma \equiv \gamma_{12}/\gamma_{13} = 0.9$, $\delta\omega_c = 0$, $\bar{n}_{ij} = 0$, $\Omega_c = 0.56$, and $\Omega_p = 0.50$. All the frequencies are scaled with $\gamma_{13} (\approx 0.62 \times 10^8 \text{ s}^{-1})$.

tating wave approximations (RWA), the dynamics of the Λ -system is described by the following Lindblad-type evolution equation of a 3×3 reduced density matrix $\rho(t)$ (see Supplemental Material),

$$\partial_t \rho(t) = -(i/\hbar)[H_S + H_{\text{int}}, \rho(t)] + \mathcal{D}(\rho(t)) \quad (1)$$

where $H_S = \hbar(\omega_1|1\rangle\langle 1| + \omega_2|2\rangle\langle 2| + \omega_3|3\rangle\langle 3|)$ with $\hbar\omega_i$ denoting the energy level of the i -th state, and $\mathcal{D}(\rho(t))$ is the Lindblad dissipator.

Equation (1) can be transformed to $\partial_t \tilde{\rho}(t) = \mathcal{L}\tilde{\rho}(t)$ where $\tilde{\rho} \equiv (\tilde{\rho}_{11}, \tilde{\rho}_{12}, \tilde{\rho}_{13}, \tilde{\rho}_{21}, \tilde{\rho}_{22}, \tilde{\rho}_{23}, \tilde{\rho}_{31}, \tilde{\rho}_{32}, \tilde{\rho}_{33})^T$ is the vector notation unraveling the individual elements of $\rho(t)$ transformed into those in the rotating frame (with the symbol $\tilde{\cdot}$ indicating the rotating frame), and \mathcal{L} is the Liouvillian super-operator expressed as 9×9 matrix in Fock-Liouville space [23]. The steady-state value of each element $\tilde{\rho}_{ij}^{ss}$ is calculated from $\mathcal{L}\tilde{\rho}^{ss} = 0$ (see Eq. (S26) in SM). Fig. 1 shows the population in each state ($\tilde{\rho}_{ii}^{ss}$, which satisfies $\sum_{i=1,2,3} \tilde{\rho}_{ii}^{ss} = 1$) and coherences between the states $|i\rangle$ and $|j\rangle$ ($\tilde{\rho}_{ij}^{ss} = \rho_{ij}^R + i\rho_{ij}^I$, $i \neq j$, with $\rho_{ij}^R \equiv \text{Re}\{\tilde{\rho}_{ij}^{ss}\}$ and $\rho_{ij}^I \equiv \text{Im}\{\tilde{\rho}_{ij}^{ss}\}$) as a function of the detuning frequency of the probe pulse ($\delta\omega_p$).

At two-photon resonance ($\delta\omega_p = \delta\omega_c = 0$) and $\Omega_c \approx \Omega_p$, the atom is locked in the states $|2\rangle$ and $|3\rangle$, without populating the state $|1\rangle$, i.e., $\tilde{\rho}_{22}, \tilde{\rho}_{33} \neq 0$ but $\tilde{\rho}_{11} = 0$ (panel (a) of Fig. 1B). In addition, except for the real part of coherence between $|2\rangle$ and $|3\rangle$ ($\rho_{23}^R \neq 0$), all the coherence terms vanish, $\rho_{12}^R = \rho_{12}^I = \rho_{13}^R = \rho_{13}^I = \rho_{23}^I = 0$. This situation corresponds to the CPT, where the effects of control and probe pulses are cancelled off via destructive inter-

ference, and the atomic state is delocalized between $|2\rangle$ and $|3\rangle$, forming a dark state. Since there is neither dispersion ($\rho_{13}^R = 0$) nor absorption of light ($\rho_{13}^I = 0$), the atomic media look effectively transparent to the probe pulse.

Transition current, fluctuations, and Fano factor. Laser pulse applied to the system for a time interval sufficiently longer than the decay time ($\tau \equiv \gamma_{13}t \gg 1$) establishes steady-state current of photon absorption and emission. With the net number of photon (or atomic) transitions in the Λ -system denoted as $n(\tau)$, where $n(\tau) > 0$ is for emissions and $n(\tau) < 0$ is for absorptions, the photon current at steady state, its fluctuations, and the corresponding Fano factor are defined as follows.

$$\begin{aligned} \langle j \rangle &\equiv \lim_{\tau \gg 1} \frac{\langle n(\tau) \rangle}{\tau}, \\ \text{var}[j] &\equiv \lim_{\tau \gg 1} \frac{\text{var}[n(\tau)]}{\tau}, \\ \mathcal{F} &= \lim_{\tau \gg 1} \frac{\text{var}[n(\tau)]}{\langle n(\tau) \rangle} = \frac{\text{var}[j]}{\langle j \rangle}. \end{aligned} \quad (2)$$

Detailed expressions of these for the Λ -system can be obtained by employing the method of cumulant generating function [18, 24] (see SM).

When the two energy gaps are identical ($\omega_{12} = \omega_{13} = \omega_0$), the mean thermal photon number of the bosonic bath is given by $\bar{n}_{12} = \bar{n}_{13} = \bar{n} = (e^{\beta\hbar\omega_0} - 1)^{-1}$. Then, \mathcal{F} simplifies to (see SM)

$$\mathcal{F} = \coth\left(\frac{\mathcal{A}}{2}\right) [1 + \mathcal{R} - \mathcal{I} + q(\cdot)], \quad (3)$$

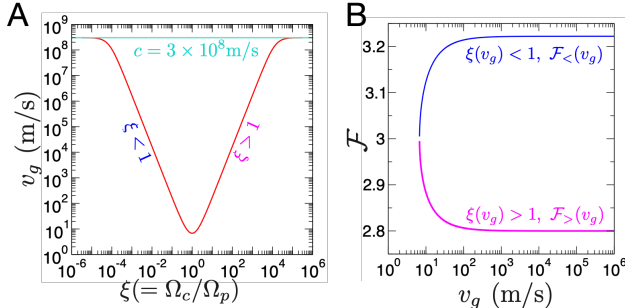


FIG. 2. Group velocity (v_g) and Fano factor (\mathcal{F}). (A) $v_g = v_g(\xi)$ in red, and vacuum speed of light c in blue. (B) \mathcal{F} versus v_g calculated by varying $\xi (= \Omega_c/\Omega_p)$ at two-photon resonance ($\delta\omega_p = \delta\omega_c = 0$). Depending on whether $\xi < 1$ or $\xi > 1$, \mathcal{F} changes differently with v_g . For the calculation, the parameters were taken from Hau *et al.* [1] that experimented on ^{23}Na atom: $\bar{n}_{ij} = 0$ ($\mathcal{A} \gg 1$), $\gamma (\equiv \gamma_{12}/\gamma_{13}) = 0.9$, and $\mathcal{N} = 2\pi N_d(\omega_p/\Omega_p) \approx 1.78 \times 10^8$, which is estimated from $N_d = N|\vec{d}_{13}|^2/(\hbar\Omega_p\gamma_{13}) = 0.11$ with $N \approx 8 \times 10^{13} \text{ cm}^{-3}$, $|\vec{d}_{13}| \approx 1.4 \times 10^{-29} \text{ C}\cdot\text{m} \approx 4.2 \times 10^{-18} \text{ statC}\cdot\text{cm}$, $\Omega_p = 0.2$ [25], $\gamma_{13} \approx 0.62 \times 10^8 \text{ s}^{-1} = (16.23 \text{ ns})^{-1}$, and $\omega_p = (2\pi c/\lambda_p)/\gamma_{13} \approx 2\pi \times 8.21 \times 10^6$ with $\lambda_p \approx 589 \text{ nm}$.

where $\mathcal{A} = \beta\hbar\omega_0$, $\mathcal{R} \equiv 2\sum_{i \neq j}(\rho_{ij}^R)^2$, $\mathcal{I} \equiv 6\sum_{i \neq j}(\rho_{ij}^I)^2$ with $i, j \in \{1, 2, 3\}$, and $q(\cdot) = q(\Omega_c, \Omega_p, \gamma, \mathcal{A}, \delta\omega_c, \delta\omega_p)$. Similarly to the Fano factor for the field-driven TLS [22], \mathcal{F} of the Λ -system is determined by the competition between the real (\mathcal{R}) and imaginary (\mathcal{I}) parts of steady-state coherence; however, there is an additional factor $q(\cdot)$ in the expression (Eq.(3)), which is absent in the TLS but could be significant in determining the magnitude of \mathcal{F} for the Λ -system. The full expression of $q(\cdot)$ is rather complicated, but at two-photon resonance it is greatly simplified to

$$q(\cdot) = \frac{2(\gamma\xi^6 + 2\gamma\xi^4 + 2\xi^2 + 1)}{(\xi^2 + 1)(\xi^2 + \gamma)^2} \quad (4)$$

where $\xi (\equiv \Omega_c/\Omega_p)$ is the experimentally controllable variable, and $\gamma \equiv \gamma_{12}/\gamma_{13}$ (see Eqs. (S29) and (S30)). Note that the result of TLS, i.e., $q(\cdot) = 0$ is recovered under the limiting condition of $\gamma \gg 1$.

Group velocity of probe field and Fano factor. A change in the refractive index gives rise to a change in the group velocity $v_g = [dk(\omega)/d\omega]^{-1}$. Since $k(\omega) = \omega\eta(\omega)/c$ where $\eta(\omega)$ is the real part of refractive index and c is the vacuum speed of light, the group velocity

of probe field across the medium is given by (see SM)

$$v_g = c \left(\eta(\omega) + \omega \frac{d\eta(\omega)}{d\omega} \right)^{-1} = \frac{c}{1 + 2\pi N_d \rho_{13}^R + 2\pi\omega_p N_d (\partial\rho_{13}^R/\partial\omega_p)}. \quad (5)$$

where $N_d \equiv N|\vec{d}_{13}|/\zeta_p (= N|\vec{d}_{13}|^2/\hbar\Omega_p\gamma_{13})$ with N being the density of atoms comprising the medium of atomic vapor.

The condition of two-photon resonance ($\delta\omega_p = \delta\omega_c = 0$) simplifies Eq. (5) with $(\rho_{13}^R)_{\delta\omega_p=0} = 0$ (Fig. 1B, Fig. 3A inset, and see Eq. (S26)). Hence, the group velocity is greatly reduced by increasing the derivative term, $(\partial\rho_{13}^R/\partial\omega_p)_{\delta\omega_p=0}$, namely, by increasing the variation of refractive index involving the states $|1\rangle$ and $|3\rangle$ with the probe frequency [1]. In fact, it is straightforward to show $(\partial\rho_{13}^R/\partial\omega_p)_{\delta\omega_p=0} = \Omega_p^{-1}(\rho_{23}^R)_{\delta\omega_p=0}^2$ (Eq. S26). Thus, the group velocity is determined by the strength of Raman coherence, namely, the magnitude of the real part of coherence between the two ground states $|2\rangle$ and $|3\rangle$ at $\delta\omega_p = 0$ as follows.

$$v_g = \frac{c}{1 + \mathcal{N}(\rho_{23}^R)_{\delta\omega_p=0}^2}, \quad (6)$$

where $\mathcal{N} \equiv 2\pi N_d\omega_p/\Omega_p$ is a dimensionless factor determined by the density of atoms comprising the medium, the magnitude of the transition dipole moment $|\vec{d}_{13}|$, the resonant and Rabi frequencies, ω_p and Ω_p .

The relationship between v_g and \mathcal{F} for Λ -systems can be identified through ξ (see Fig. 2A for $v_g = v_g(\xi)$). Fig. 2B shows a curve of \mathcal{F} versus v_g parameterized with ξ at $\delta\omega_p = \delta\omega_c = 0$ for $\gamma = 0.9$, which clarifies a trade-off relation between \mathcal{F} and v_g for experimentally relevant range of variable, $\xi > 1$. It is noteworthy that the Fano factor of photon transitions sharply increase to $\mathcal{F} \simeq 3$ when the group velocity of light reaches its minimal value $v_g \simeq 7 \text{ m/s}$ (Fig. 2B, magenta line), which is even smaller than the experimentally reported value.

For $\mathcal{A} \gg 1$ (or $\bar{n} \sim 0$) with $\delta\omega_c = \delta\omega_p = 0$, the expressions of coherence terms (Eq. S26) are greatly simplified, enabling us to further clarify a relationship between v_g and \mathcal{F} . With $(\rho_{23}^R)_{\delta\omega_p=0}^2 = \xi^2/(\xi^2 + 1)^2$, $\rho_{23}^I = \rho_{12}^R = \rho_{12}^I = \rho_{13}^R = \rho_{13}^I = 0$ (Eq. (S26)) and $q(\cdot)$ in Eq. (4), the group velocity and the Fano factor read

$$v_g = \frac{c}{\mathcal{N}} \frac{1}{1 + \frac{1}{(\xi + 1/\xi)^2}} \quad (7)$$

and

$$\mathcal{F} \simeq 1 + \frac{2(1 + \gamma\xi^2)}{(\gamma + \xi^2)}. \quad (8)$$

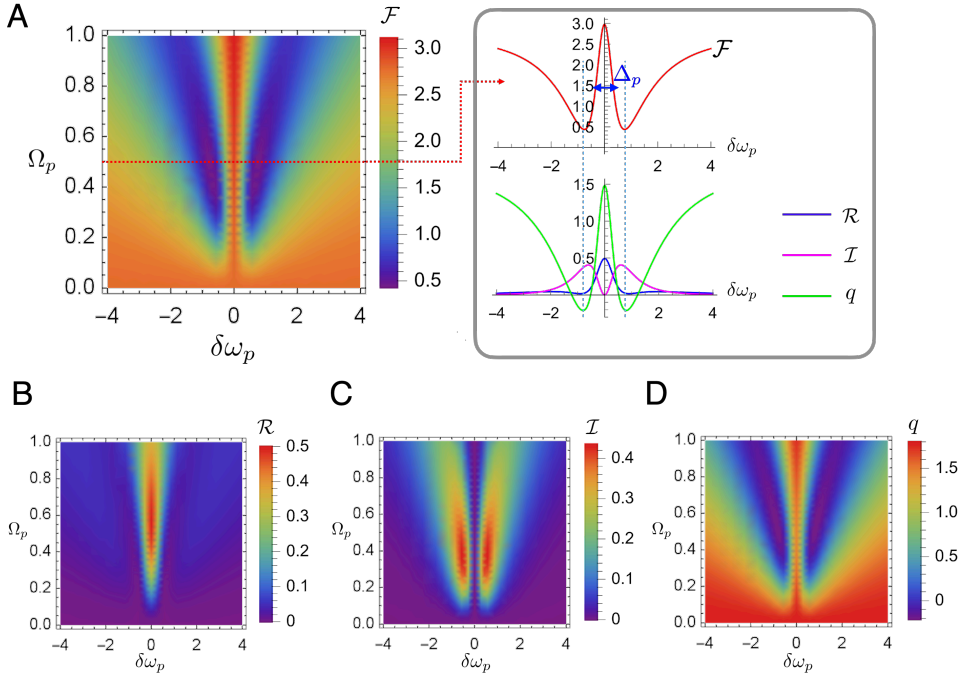


FIG. 3. Effect of detuning. (A) Diagram of $\mathcal{F}(\delta\omega_p, \Omega_p)$ calculated for $\delta\omega_c = 0$ with $\Omega_c = 0.56$, $\gamma = 0.90$, $\mathcal{A} = 47$. (Inset) \mathcal{F} , \mathcal{R} , \mathcal{I} , and q as a function of $\delta\omega_p$ for $\Omega_p = 0.5$. The blue vertical dashed line indicates the value of $\delta\omega_p (\approx 0.8)$ that gives rise to the minimal \mathcal{F} . The range of transparency window (Δ_p) is indicated by the arrow. (B) Real (\mathcal{R}) and (C) imaginary parts of coherence (\mathcal{I}) and (D) the factor q as a function of probe detuning $\delta\omega_p$ and driving frequency Ω_p .

From Eq. (7), it is clear that v_g minimizes to $v_g = c/(1 + \mathcal{N}/4)$ for $\xi = 1$, and saturates to $v_g = c$ for $\xi \gg \sqrt{\mathcal{N}}$ or $\xi \ll 1/\sqrt{\mathcal{N}}$ (see Fig. 2A). Next, insertion of the two solutions of Eq. (7), $\xi(v_g) = \frac{1}{2}[\sqrt{\mathcal{N}/(c/v_g - 1)} \pm \sqrt{\mathcal{N}/(c/v_g - 1) - 4}]$, to Eq. (8) yields $\mathcal{F} = \mathcal{F}_>(v_g)$ for $\xi(v_g) > 1$ (magenta line in Fig. 2B), and $\mathcal{F} = \mathcal{F}_<(v_g)$ for $\xi(v_g) < 1$ (blue line in Fig. 2B). We note that the condition of $\xi(v_g) > 1$ is of more practical relevance to the slow-light experiment because the current fluctuations are smaller and more controllable with $\mathcal{F}_>(v_g) \leq 3$. At $\xi(v_g) = 1$ or equivalently at the slowest velocity $v_g = c/(1 + \mathcal{N}/4)$, one always obtains $\mathcal{F} = 3$.

For more general case with $\delta\omega_p \neq 0$ and $\delta\omega_c = 0$, the expression of \mathcal{F} is complicated; yet, \mathcal{F} is still an even function of $\delta\omega_p$ (Eq. (S26)). Confining ourselves to the condition $\xi > 1$, we resort to numerics to calculate $\mathcal{F}(\delta\omega_p, \Omega_p)$ (Fig. 3), finding that \mathcal{F} is maximized over the transparency window Δ_p , given by $\Delta_p \sim \left[\partial \rho_{13}^R / \partial \delta\omega_p \Big|_{\delta\omega_p=0} \right]^{-1} = \Omega_p(\xi^2 + 1)^2 / \xi^2$. Note that Δ_p is narrow for the case of CPT ($\xi \approx 1$) but is wide for EIT ($\xi \gg 1$). Over the Δ_p , $\rho_{13}^R, \rho_{13}^I \approx 0$ (Fig. 1B), and \mathcal{R} and q display maximal contribution at two-photon resonance (Fig. 3A inset, and B, D), whereas $\mathcal{I} \approx 0$, i.e., the absorption is negligible

(Fig. 3A inset and C).

Notably, maximal suppression of the current fluctuations, resulting in $\mathcal{F} < 1$, is identified under a detuning condition $\delta\omega_p \neq 0$ where \mathcal{I} is maximized, $\mathcal{R} \approx 0$, and $q < 0$ (Fig. 3A inset, B, and D); however, the value of $\delta\omega_p$ is beyond the transparency window, which is not suitable for generation of absorption-free slow light. This condition corresponds to the absorption doublet [26] involving the transitions from $|0\rangle$ to two eigenstates $|\pm\rangle$ comprised of the three electronic states $|1\rangle$, $|2\rangle$, and $|3\rangle$ (see Fig. S1B and Eq. (S5)).

Concluding Remarks. This work has established a fundamental trade-off between the group velocity of light and photon fluctuations for the Λ -type three-level system. In particular, the Fano factor of net number of photon transitions $n(\tau)$, which dictates the fluctuations of the laser power as $\langle(\delta n(\tau))^2\rangle \propto \langle(\delta I)^2\rangle$, is maximized to $\mathcal{F} = 3 \coth(\mathcal{A}/2)$ at the lowest group velocity, $v_g \approx (4/\mathcal{N})c$. This indicates that slow light is attained at the expense of fluctuations of the irreversible photon current. This trade-off, which may be inevitable in the basic setup of CPT or EIT-based optical quantum memory device, is physically sensible in that as the velocity of light is reduced, overall fluctuations in the photon current is enhanced over the prolonged travel time of the photon inside the medium.

At two-photon resonance, the real part of coherence between the two ground states (ρ_{23}^R), which engenders slow light (Eq. (7)) and enhanced fluctuations of signal (Eq. (3)), is maximized at the regime corresponding to CPT, where the Rabi frequencies of control and probe pulses are identical ($\xi = \Omega_c/\Omega_p = 1$).

Our results can also be applied to the medium consisting of ^{133}Cs atoms, whose $D1$ line constitutes the three-level Λ -system. For Cs atoms, the frequency gap between the two ground states $6^2S_{1/2}(|F=3\rangle)$ and $6^2S_{1/2}(|F=4\rangle)$, where F stands for the total angular momentum quantum number, is ~ 9.2 GHz. The condition of $\rho_{23}^R \neq 0$ and $\rho_{23}^I = 0$ signifies a Raman coherence between $|F=3\rangle$ and $|F=4\rangle$ effectively with no absorption. The slowest group velocity achievable for the case of CPT regime ($\xi \approx 1$) of ^{133}Cs vapor [27] is $v_g \approx 38$ m/s with $\mathcal{N} = 2\pi N_d(\omega_p/\Omega_p) \approx 3.2 \times 10^7$, which is estimated from $\Omega_p = 0.5$, $\omega_p = (2\pi c/\lambda_p)/\gamma_{13} \approx 2.1 \times 10^7$ with $\lambda_p \approx 894$ nm [27] and $\gamma_{13} \approx 10^8$ s $^{-1}$, and $N_d = N|\vec{d}_{13}|^2/(\hbar\Omega_p\gamma_{13}) = 0.12$ with $N \approx 10^{12}$ cm $^{-3}$ and $|\vec{d}_{13}| = 2.7 \times 10^{-29}$ C \cdot m = 8.09×10^{-18} statC \cdot cm [28]. Our estimate for the slowest group velocity of light in the atomic vapor of cesium is amenable for an experimental verification.

Finally, we emphasize that the size of current fluctuations (or noise level) of three-level Λ -system at the slowest group velocity is universal ($\mathcal{F} = 3$) regardless of the atomic type, which warrants experimental confirmation. The formalism of this work can be extended to other configurations of EIT/CPT for quantum memory device adopting the vee and ladder structures [6] or even to Bose-Einstein condensates [3], which would help to understand new fundamental trade-offs and to develop practical ways to utilize them.

We thank Prof. Hyukjoon Kwon for careful reading of the manuscript and helpful discussions. This work was supported by the KIAS Individual Grants (CG077602 to DS, and CG035003 to CH) from the Korea Institute for Advanced Study, and by the US National Science Foundation (CHE-1900170 to SJJ). We thank the Center for Advanced Computation in KIAS for providing computing resources.

* hyeoncb@kias.re.kr

- [1] L. V. Hau, S. E. Harris, Z. Dutton, and C. H. Behroozi, Light speed reduction to 17 metres per second in an ultracold atomic gas, *Nature* **397**, 594 (1999).
- [2] D. Budker, D. Kimball, S. Rochester, and V. Yashchuk, Nonlinear magneto-optics and reduced group velocity of light in atomic vapor with slow ground state relaxation, *Phys. Rev. Lett.* **83**, 1767 (1999).
- [3] N. S. Ginsberg, S. R. Garner, and L. V. Hau, Coherent control of optical information with matter wave dynamics, *Nature* **445**, 623 (2007).
- [4] T. Baba, Slow light in photonic crystals, *Nature photonics* **2**, 465 (2008).
- [5] A. I. Lvovsky, B. C. Sanders, and W. Tittel, Optical quantum memory, *Nature photonics* **3**, 706 (2009).
- [6] L. Ma, O. Slattery, and X. Tang, Optical quantum memory based on electromagnetically induced transparency, *J. Opt.* **19**, 043001 (2017).
- [7] T. Goldzak, A. A. Mailybaev, and N. Moiseyev, Light stops at exceptional points, *Phys. Rev. Lett.* **120**, 013901 (2018).
- [8] W. Li, P. Islam, and P. Windpassinger, Controlled transport of stored light, *Phys. Rev. Lett.* **125**, 150501 (2020).
- [9] H. Gray, R. Whitley, and C. Stroud, Coherent trapping of atomic populations, *Opt. Lett.* **3**, 218 (1978).
- [10] K.-M. C. Fu, C. Santori, C. Stanley, M. Holland, and Y. Yamamoto, Coherent population trapping of electron spins in a high-purity n-type GaAs semiconductor, *Phys. Rev. Lett.* **95**, 187405 (2005).
- [11] S. E. Harris, Electromagnetically induced transparency, *Phys. Today* **50**, 36 (1997).
- [12] M. T. Hsu, G. Hetet, O. Gloeckl, J. J. Longdell, B. C. Buchler, H.-A. Bachor, and P. K. Lam, Quantum study of information delay in electromagnetically induced transparency, *Phys. Rev. Lett.* **97**, 183601 (2006).
- [13] D. H. Meyer, C. O'Brien, D. P. Fahey, K. C. Cox, and P. D. Kunz, Optimal atomic quantum sensing using electromagnetically-induced-transparency readout, *Phys. Rev. A* **104**, 043103 (2021).
- [14] U. Seifert, Stochastic Thermodynamics, Fluctuation Theorems and Molecular Machines, *Rep. Prog. Phys.* **75**, 126001 (2012).
- [15] J. M. Horowitz and T. R. Gingrich, Thermodynamic uncertainty relations constrain non-equilibrium fluctuations, *Nat. Phys.* **16**, 15 (2020).
- [16] Y. Song and C. Hyeon, Thermodynamic uncertainty relation to assess biological processes, *J. Chem. Phys.* **154**, 130901 (2021).
- [17] M. Esposito, U. Harbola, and S. Mukamel, Nonequilibrium fluctuations, fluctuation theorems, and counting statistics in quantum systems, *Rev. Mod. Phys.* **81**, 1665 (2009).
- [18] M. Bruderer, L. D. Contreras-Pulido, M. Thaller, L. Sironi, D. Obreschkow, and M. B. Plenio, Inverse counting statistics for stochastic and open quantum systems: the characteristic polynomial approach, *New J. Phys.* **16**, 033030 (2014).
- [19] J. Liu and D. Segal, Thermodynamic uncertainty relation in quantum thermoelectric junctions, *Phys. Rev. E* **99**, 062141 (2019).
- [20] Y. Hasegawa, Thermodynamic uncertainty relation for general open quantum systems, *Phys. Rev. Lett.* **126**, 010602 (2021).
- [21] P. Menczel, E. Loisa, K. Brandner, and C. Flindt, Thermodynamic uncertainty relations for coherently driven open quantum systems, *J. Phys. A: Math.*

Theor. **54**, 314002 (2021).

[22] D. Singh and C. Hyeon, Origin of loose bound of the thermodynamic uncertainty relation in a dissipative two-level quantum system, Phys. Rev. E **104**, 054115 (2021).

[23] D. Manzano, A short introduction to the Lindblad master equation, AIP Adv. **10**, 025106 (2020).

[24] C. Flindt, T. Novotný, A. Braggio, and A.-P. Jauho, Counting statistics of transport through coulomb blockade nanostructures: High-order cumulants and non-markovian effects, Phys. Rev. B **82**, 155407 (2010).

[25] D. A. Steck, Sodium D Line Data (2003).

[26] M. O. Scully and M. S. Zubairy, *Quantum Optics* (Cambridge University Press, 1997).

[27] D. Höckel and O. Benson, Electromagnetically induced transparency in cesium vapor with probe pulses on the single-photon level, Phys. Rev. Lett. **105**, 153605 (2010).

[28] D. A. Steck, Cesium D Line Data (2003).

[29] H. J. Carmichael, *Statistical Methods in Quantum optics 1* (Springer, 2002).

[30] M. Bruderer, L. D. Contreras-Pulido, M. Thaller, L. Sironi, D. Obreschkow, and M. B. Plenio, Inverse counting statistics for stochastic and open quantum systems: the characteristic polynomial approach, New J. Phys. **16**, 033030 (2014).

[31] J. Wu, F. Liu, J. Ma, R. J. Silbey, and J. Cao, Efficient energy transfer in light-harvesting systems: Quantum-classical comparison, flux network, and robustness analysis, J. Chem. Phys. **137**, 174111 (2012).

SUPPLEMENTAL MATERIAL

Coherent population trapping (CPT) and electromagnetically induced transparency (EIT)

CPT. The absorption and dispersion profiles of probe pulse as a function of detuning ($\delta\omega_p$) are calculated in Fig. 1B. At the two-photon resonance ($\delta\omega_p = \delta\omega_c = 0$), both the coherences between the states $|1\rangle$ and $|3\rangle$ and between the states $|1\rangle$ and $|2\rangle$ vanish ($\rho_{13}^R = \rho_{13}^I = 0$ and $\rho_{12}^R = \rho_{12}^I = 0$ in Fig. 1B), which implies that the medium is effectively transparent to the probe and control pulses. The two light pulses interacting with the matter vanish via the destructive interference between two pathways between $|3\rangle \leftrightarrow |1\rangle \rightarrow |2\rangle$ and $|2\rangle \leftrightarrow |1\rangle \rightarrow |3\rangle$ (Fig. S1A).

To show the destructive quantum interference more explicitly, we consider an addition of two pulses with quantum coherence,

$$\tilde{\rho}_{\text{sum}} = \tilde{\rho}_{12} + \tilde{\rho}_{13}. \quad (\text{S1})$$

Note that $\tilde{\rho}_{ij} = |\tilde{\rho}_{ij}| \exp(i\theta_{ij})$ with $|\tilde{\rho}_{ij}|^2 = (\rho_{ij}^R)^2 + (\rho_{ij}^I)^2$ and $\tan \theta_{ij} = (\rho_{ij}^I / \rho_{ij}^R)$. Numerical calculation using the results in Eq. (S26) gives rise to Fig. S2, and shows that the amplitude of $\tilde{\rho}_{\text{sum}}$ vanishes at two-photon resonance ($\delta\omega_p = \delta\omega_c = 0$). Thus, the excitation transfer to the state $|1\rangle$ is negligible, and almost all the atomic population is trapped in the states $|2\rangle$ and $|3\rangle$ (Fig. 1A). The “coherent population trapping” (CPT) refers to such a trapping of population in the two ground states via a coherent superposition of the quantum states.

The destructive interference and hence population trapping in states $|2\rangle$ and $|3\rangle$ results in strong coupling between these states, which is reflected in the high value of ρ_{23}^R (see Fig. 1B).

More complete physical interpretation of CPT can be given in terms of the basis representing the dressed (or eigen) states. Under the following unitary transformation, which is equivalent to describing the system

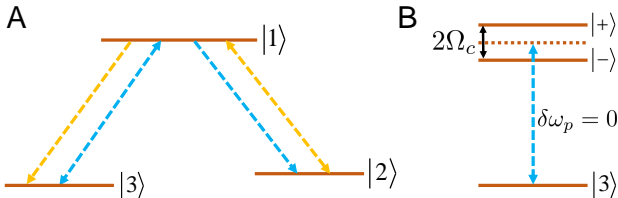


FIG. S1. (A) Bare state basis to show the paths involved in the destructive interference and (B) the corresponding dressed state picture for the weak probe field.

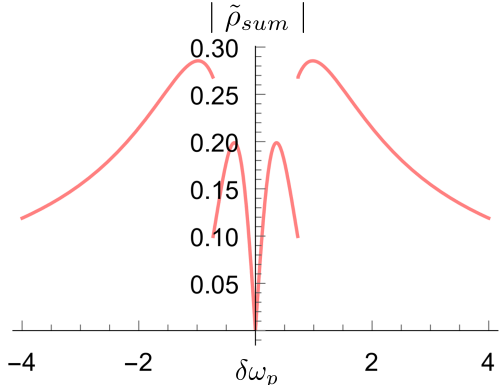


FIG. S2. Plot of $|\tilde{\rho}_{\text{sum}}| = |\tilde{\rho}_{12} + \tilde{\rho}_{13}|$ with varying $\delta\omega_p$ with fixed $\delta\omega_c = 0$ for $\Omega_c = 0.56$, $\Omega_p = 0.50$, $\gamma = 0.9$, $\bar{n}_{ij} = 0$.

in the rotating frame,

$$|\psi\rangle = \mathcal{U}|\phi\rangle, \quad (\text{S2})$$

where $\mathcal{U} = e^{-i\omega_p t|1\rangle\langle 1| - i(\omega_p - \omega_c)t|2\rangle\langle 2|}$, the Schrödinger equation $\partial_t |\psi\rangle = -iH/\hbar |\psi\rangle$ is written as $\partial_t |\phi\rangle = -iH_{\text{eff}}/\hbar |\phi\rangle$ with

$$\begin{aligned} H_{\text{eff}} &= \mathcal{U}^\dagger H \mathcal{U} - i\hbar \mathcal{U}^\dagger \frac{d\mathcal{U}}{dt} \\ &= -\hbar\delta\omega_p |1\rangle\langle 1| - \hbar(\delta\omega_p - \delta\omega_c) |2\rangle\langle 2| \\ &\quad - \hbar(\Omega_p |1\rangle\langle 3| + \Omega_c |1\rangle\langle 2| + h.c.). \end{aligned} \quad (\text{S3})$$

When $\delta\omega_p = \delta\omega_c = \delta\omega$ is assumed for simplicity, the energy eigenvalues and eigenstates of H_{eff} are

$$\begin{aligned} \bar{\lambda}_0 &= 0 \\ \bar{\lambda}_\pm &= 0.5\hbar \left(\delta\omega \pm \sqrt{\delta\omega^2 + 4(\Omega_p^2 + \Omega_c^2)} \right), \end{aligned} \quad (\text{S4})$$

and

$$\begin{aligned} |0\rangle &= \cos\theta |3\rangle - \sin\theta |2\rangle, \\ |-\rangle &= \sin\theta \cos\phi |3\rangle + \cos\theta \cos\phi |2\rangle - \sin\phi |1\rangle, \\ |+\rangle &= \sin\theta \sin\phi |3\rangle + \cos\theta \sin\phi |2\rangle + \cos\phi |1\rangle, \end{aligned} \quad (\text{S5})$$

where the mixing angles θ and ϕ are defined as

$$\begin{aligned} \theta &= \tan^{-1}(\Omega_p/\Omega_c) \\ \phi &= 0.5 \tan^{-1} \left(2\sqrt{\Omega_p^2 + \Omega_c^2} / \delta\omega \right). \end{aligned} \quad (\text{S6})$$

Under the two-photon resonance condition ($\delta\omega = 0$), the eigenstate $|0\rangle$, a coherent superposition between the states $|2\rangle$ and $|3\rangle$, of the effective Hamiltonian (Eq. (S3)) has zero eigenvalue. Hence, the state $|0\rangle$ is a *dark state* that does not evolve with time, and is decoupled from the applied fields. Now the spontaneous emission from the state $|1\rangle$ always populates the

quantum states $|2\rangle$ and $|3\rangle$. Therefore, irrespective of the initial condition, the atomic population is trapped in the dark state $|0\rangle$ for an extended period of time, $t \gg 1/\gamma$. This corresponds to the CPT.

EIT. For a strong control field ($\xi = \Omega_c/\Omega_p \gg 1$) and $\delta\omega = 0$, a coherent superposition of states $|1\rangle$ and $|2\rangle$, produces the dressed states $|\pm\rangle$, without affecting the state $|3\rangle$ ($= |0\rangle$) (Fig. S1B). The three energy eigen-states and corresponding eigenvalues (inside parenthesis) are obtained as

$$\begin{aligned} |0\rangle &= |3\rangle \quad (\bar{\lambda}_0 = 0), \\ |\pm\rangle &= \frac{1}{\sqrt{2}} (|2\rangle \pm |1\rangle) \quad (\bar{\lambda}_\pm = \pm\hbar\Omega_c). \end{aligned} \quad (S7)$$

In this case, the transition amplitude at the resonant probe frequency ($\delta\omega_p = 0$) between the ground state $|0\rangle = |3\rangle$ to the dressed states $|\pm\rangle$ can be written as $\langle 3 | \vec{d} | + \rangle + \langle 3 | \vec{d} | - \rangle \simeq \vec{d}_{32} + \vec{d}_{31} + \vec{d}_{32} - \vec{d}_{31} = 2\vec{d}_{32} = 0$ because the electric dipole selection rule that disallows the transition from $|2\rangle \rightarrow |3\rangle$ ($\vec{d}_{32} = 0$). Consequently, all the population is effectively confined in the dark state $|0\rangle$. At $\delta\omega_p = 0$, the media is transparent to the pulse, and does not absorb the probe pulse. This strong control field-induced ($\Omega_c \gg \Omega_p$) conversion of an absorptive medium to a transparent one is termed the electromagnetically induced transparency (EIT) [26]. The EIT creates the destructive interference between the transition pathways $|3\rangle \rightleftharpoons |1\rangle$ and $|2\rangle \rightleftharpoons |1\rangle \rightarrow |3\rangle$.

The energy gap between the dressed states is $2\hbar\Omega_c$. Then, the conditions for the perfect resonance between $|0\rangle$ and $|\pm\rangle$ appears when $\delta\omega_p = \pm\Omega_c$, resulting in the complete absorption of probe pulse, giving rise to the Aulter-Townes absorption doublet [26]. The off-resonant probe pulse ($\delta\omega_p \approx 1$) engenders the absorption doublet where again the dispersion becomes zero ($\rho_{13}^R = 0$), but this time the absorption (ρ_{13}^I) is maximized.

The relation between the linear susceptibility of media and the quantum coherence

The probe pulse-induced polarization of the Λ -system is quantified with the dipole moment between $|1\rangle$ and $|3\rangle$ per unit volume as $\vec{P}_{13} = N\langle\vec{d}_3\rangle = \chi_{13}\vec{E}_p$, where N is the number density of atoms. $\vec{P}_{13} = \hat{e}_p\zeta_p\chi_{13}e^{-i\omega_p t} + c.c.$, where χ_{13} is the linear susceptibility of the medium [26]. Since $\langle\vec{d}_3\rangle = \text{Tr}(\tilde{\rho}\vec{d}) = \tilde{\rho}_{13}\vec{d}_{31} + \tilde{\rho}_{31}\vec{d}_{13} = \rho_{13}e^{i\omega_p t}\vec{d}_{31} + \rho_{31}e^{-i\omega_p t}\vec{d}_{13} \simeq e^{i\omega_p t}\rho_{13}\vec{d}_{31} = \tilde{\rho}_{13}\vec{d}_{31}$, the linear susceptibility can be expressed as $\chi_{13} = |\vec{P}_{13}|/|\vec{E}_p| = N_d\tilde{\rho}_{13}$ with $N_d \equiv N|\vec{d}_{31}|/\zeta_p$. For

the medium with $|\chi_{13}| \ll 1$, the refractive index, dielectric constant and linear susceptibility for the probe field are related with one another in Gaussian units as

$$\begin{aligned} \eta_{13} (= \sqrt{\epsilon_{13}}) &= \sqrt{1 + 4\pi\chi_{13}} \\ &\simeq 1 + 2\pi\chi_{13}^R + i2\pi\chi_{13}^I. \end{aligned} \quad (S8)$$

where χ^R and χ^I are the real and imaginary parts of the susceptibility. When the probe field, $\vec{E}_p \sim e^{ik_p z} \sim e^{i\beta z}e^{-\alpha z/2}$, passes across the dielectric medium with a wave vector k_p ,

$$\begin{aligned} k_p &= \frac{\omega_p}{c}\eta_{13} \\ &= \underbrace{\frac{\omega_p}{c}(1 + 2\pi\chi_{13}^R)}_{=\beta} + \underbrace{\frac{i}{2}\frac{\omega_p}{c}4\pi\chi_{13}^I}_{=\alpha}, \end{aligned} \quad (S9)$$

it moves through the medium with a phase velocity $c/(1 + 2\pi\chi_{13}^R)$, and is also attenuated by the medium with an absorption coefficient α . Since $\chi_{13} = N_d\tilde{\rho}_{13}$, the real and imaginary parts of the susceptibility is linked to the dispersion and absorption profiles of the medium, respectively, as $\chi_{13}^R = N_d\rho_{13}^R$ and $\chi_{13}^I = N_d\rho_{13}^I$.

Evolution equation

The total Hamiltonian in the presence of an external field is expressed as [26, 29]

$$H = H_S + H_{\text{int}} + H_B + H_{SB}, \quad (S10)$$

where

$$\begin{aligned} H_S &= \hbar(\omega_1|1\rangle\langle 1| + \omega_2|2\rangle\langle 2| + \omega_3|3\rangle\langle 3|) \\ H_{\text{int}} &= -\vec{d}_2 \cdot \vec{E}_c - \vec{d}_3 \cdot \vec{E}_p \\ H_B &= \sum_{\mathbf{k},\lambda} \hbar\omega_{\mathbf{k},\lambda} b_{\mathbf{k},\lambda}^\dagger b_{\mathbf{k},\lambda} \\ H_{SB} &= \sum_{\mathbf{k},\lambda} \hbar \left[(g_{\mathbf{k},\lambda}^*)_{12} b_{\mathbf{k},\lambda}^\dagger |2\rangle\langle 1| + (g_{\mathbf{k},\lambda})_{12} b_{\mathbf{k},\lambda} |1\rangle\langle 2| \right. \\ &\quad \left. + (g_{\mathbf{k},\lambda}^*)_{13} b_{\mathbf{k},\lambda}^\dagger |3\rangle\langle 1| + (g_{\mathbf{k},\lambda})_{13} b_{\mathbf{k},\lambda} |1\rangle\langle 3| \right] \end{aligned} \quad (S11)$$

The control and probe fields, $\vec{E}_\alpha(t) = \hat{e}_\alpha\zeta_\alpha(e^{i\omega_\alpha t} + e^{-i\omega_\alpha t})$ with $\alpha = c$ and p where \hat{e}_α is the unit vector representing the direction of polarization and ζ_α denotes the amplitude, interact with the Λ -system via the interaction energy Hamiltonian $H_{\text{int}} = -\vec{d}_2 \cdot \vec{E}_c - \vec{d}_3 \cdot \vec{E}_p$, inducing the excitations of $|2\rangle \rightarrow |1\rangle$ and $|3\rangle \rightarrow |1\rangle$, respectively. The transition dipole operator is given by $\vec{d} = \vec{d}_2 + \vec{d}_3 = (\vec{d}_{12}|1\rangle\langle 2| + \vec{d}_{21}|2\rangle\langle 1|) +$

$(\vec{d}_{13}|1\rangle\langle 3| + \vec{d}_{31}|3\rangle\langle 1|)$ with the dipole matrix elements, \vec{d}_{ij} . Since the transition between $|2\rangle$ and $|3\rangle$ is effectively forbidden, $\vec{d}_{23} = \vec{d}_{32} \approx 0$. The summation $\sum_{\mathbf{k},\lambda}$ extends over the wavevector \mathbf{k} and polarization λ . The symbols, $b_{\mathbf{k},\lambda}^\dagger$ and $b_{\mathbf{k},\lambda}$ denote the creation and annihilation operators of the harmonic oscillators of angular frequency ω_k constituting the reservoir. The dipole coupling constant, $(g_{\mathbf{k},\lambda})_{1j} \equiv -i\sqrt{\omega_k/2\hbar\varepsilon_0}V\hat{e}_{\mathbf{k},\lambda} \cdot \vec{d}_{1j}$ for $j \in 2, 3$, contains the information of polarization $\hat{e}_{\mathbf{k},\lambda}$, quantization volume V and vacuum permittivity ε_0 .

The density matrix for the total system, $\rho_{\text{tot}}(t)$, evolves with time, obeying the von Neumann equation, $d\rho_{\text{tot}}(t)/dt = -\frac{i}{\hbar}[H, \rho_{\text{tot}}]$. In the framework of Lindblad approach [29], the reduced density matrix after tracing out the bath degrees of freedom obeys the following evolution equation.

$$\begin{aligned} \frac{d\rho(t)}{dt} = & -\frac{i}{\hbar}[H_S + H_{\text{int}}, \rho] \\ & + \gamma_{12}(\bar{n}_{12} + 1) \left(|2\rangle\langle 1| \rho |1\rangle\langle 2| - \frac{1}{2}\{|1\rangle\langle 1|, \rho\}_+ \right) \\ & + \gamma_{12}\bar{n}_{12} \left(|1\rangle\langle 2| \rho |2\rangle\langle 1| - \frac{1}{2}\{|2\rangle\langle 2|, \rho\}_+ \right) \\ & + \gamma_{13}(\bar{n}_{13} + 1) \left(|3\rangle\langle 1| \rho |1\rangle\langle 3| - \frac{1}{2}\{|1\rangle\langle 1|, \rho\}_+ \right) \\ & + \gamma_{13}\bar{n}_{13} \left(|1\rangle\langle 3| \rho |3\rangle\langle 1| - \frac{1}{2}\{|3\rangle\langle 3|, \rho\}_+ \right), \quad (\text{S12}) \end{aligned}$$

where $\gamma_{1j} = 4\omega_{1j}^3|d_{1j}|^2/(3\hbar c^3)$ is the spontaneous decay rate from the excited state $|1\rangle$ to the ground state $|j\rangle$ ($j = 2, 3$), $\bar{n}_{1j} = (e^{\beta\hbar\omega_{1j}} - 1)^{-1}$ is the mean number of thermal photons with $\beta = 1/k_B T$, and $\{A, B\}_+ \equiv AB + BA$ denotes the anti-commutator.

After eliminating the terms violating the energy conservation [26], which amounts to taking the rotating wave approximation (RWA), the energy hamiltonian for the light-matter interaction is simplified to

$$\begin{aligned} H_{\text{int}} \simeq & -\hbar\Omega_c(e^{-i\omega_c t}|1\rangle\langle 2| + e^{i\omega_c t}|2\rangle\langle 1|) \\ & - \hbar\Omega_p(e^{-i\omega_p t}|1\rangle\langle 3| + e^{i\omega_p t}|3\rangle\langle 1|) \quad (\text{S13}) \end{aligned}$$

where $\Omega_c = \zeta_c|\hat{e}_c \cdot \vec{d}_{12}|/\hbar$ and $\Omega_p = \zeta_p|\hat{e}_p \cdot \vec{d}_{13}|/\hbar$ corresponds to the driving (Rabi) frequencies. With H_S in Eq. (S11), H_{int} in Eq. (S13), and transformations into rotating frame which lead to $\rho_{ii} \rightarrow \tilde{\rho}_{ii}$, $\rho_{12} \rightarrow \tilde{\rho}_{12}e^{-i\omega_c t}$, $\rho_{13} \rightarrow \tilde{\rho}_{13}e^{-i\omega_p t}$, and $\rho_{23} \rightarrow \tilde{\rho}_{23}e^{-i(\omega_p - \omega_c)t}$ (see the next section **Transformation to the rotating frame**), the transformed matrix elements $\tilde{\rho}_{ij}$'s

evolve with time as follows.

$$\begin{aligned} \frac{d\tilde{\rho}_{22}}{d\tau} = & \gamma(\bar{n}_{12} + 1)\tilde{\rho}_{11} + i\Omega_c\tilde{\rho}_{12} - i\Omega_c\tilde{\rho}_{21} - \gamma\bar{n}_{12}\tilde{\rho}_{22} \\ \frac{d\tilde{\rho}_{33}}{d\tau} = & (\bar{n}_{13} + 1)\tilde{\rho}_{11} + i\Omega_p\tilde{\rho}_{13} - i\Omega_p\tilde{\rho}_{31} - \bar{n}_{13}\tilde{\rho}_{33} \\ \frac{d\tilde{\rho}_{12}}{d\tau} = & -i\Omega_c\tilde{\rho}_{11} + \left[i\delta\omega_c - \frac{\gamma}{2}(2\bar{n}_{12} + 1) - \frac{(\bar{n}_{13} + 1)}{2} \right] \tilde{\rho}_{12} \\ & + i\Omega_c\tilde{\rho}_{22} + i\Omega_p\tilde{\rho}_{32} \\ \frac{d\tilde{\rho}_{13}}{d\tau} = & -i\Omega_p\tilde{\rho}_{11} + \left[i\delta\omega_p - \frac{\gamma}{2}(\bar{n}_{12} + 1) - \frac{(2\bar{n}_{13} + 1)}{2} \right] \tilde{\rho}_{13} \\ & + i\Omega_c\tilde{\rho}_{23} + i\Omega_p\tilde{\rho}_{33} \\ \frac{d\tilde{\rho}_{23}}{d\tau} = & i\Omega_c\tilde{\rho}_{13} - i\Omega_p\tilde{\rho}_{21} \\ & + \left[i(\delta\omega_p - \delta\omega_c) - \frac{(\gamma\bar{n}_{12} + \bar{n}_{13})}{2} \right] \tilde{\rho}_{23}, \quad (\text{S14}) \end{aligned}$$

where the equations are rescaled with γ_{13} , redefining the parameters and variables, such that $\tau = \gamma_{13}t$, $\gamma = \gamma_{12}/\gamma_{13}$. Hereafter, we implicitly assume that all the rates including Ω_c , Ω_p , $\delta\omega_c$, and $\delta\omega_p$ are those scaled with γ_{13} , e.g., $\Omega_c/\gamma_{13} \rightarrow \Omega_c$, $(\omega_c - \omega_{12})/\gamma_{13} \rightarrow \delta\omega_c$ and so forth. The equations for the remaining elements are obtained from the constraints $\sum_i \rho_{ii} = 1$ and $\rho_{ji} = \rho_{ij}^*$ for $i \neq j$.

Transformation to the rotating frame

The following operation transforms the state vector $|\phi\rangle$ in the rotating frame into the one in the stationary frame ($|\psi\rangle$).

$$|\psi\rangle = \mathcal{U}(t)|\phi\rangle, \quad (\text{S15})$$

with $\mathcal{U}(t) = e^{-i\omega_p t}|1\rangle\langle 1| - i(\omega_p - \omega_c)t|2\rangle\langle 2|$. Then, the density matrix $\tilde{\rho} = |\phi\rangle\langle\phi|$ in the rotating frame is transformed into the one in the stationary frame via $|\psi\rangle\langle\psi| (= \rho) = \mathcal{U}|\phi\rangle\langle\phi|\mathcal{U}^\dagger (= \mathcal{U}\tilde{\rho}\mathcal{U}^\dagger)$.

The Baker-Campbell-Hausdorff formula,

$$e^{s\hat{A}}\hat{B}e^{-s\hat{A}} = \hat{B} + \frac{s}{1!}[\hat{A}, \hat{B}] + \frac{s^2}{2!}[\hat{A}, [\hat{A}, \hat{B}]] \dots$$

enables one to rewrite the diagonal elements as $\tilde{\rho}_{jj} = \rho_{jj}$, and the off-diagonal elements as $\tilde{\rho}_{12} = \rho_{12}e^{i\omega_c t}$, $\tilde{\rho}_{13} = \rho_{13}e^{i\omega_p t}$, and $\tilde{\rho}_{23} = \rho_{23}e^{i(\omega_p - \omega_c)t}$.

The method of cumulant generating function

The elements of the reduced density matrix in Fock-Liouville space, $\tilde{\varrho} =$

$(\tilde{\rho}_{11}, \tilde{\rho}_{12}, \tilde{\rho}_{13}, \tilde{\rho}_{21}, \tilde{\rho}_{22}, \tilde{\rho}_{23}, \tilde{\rho}_{31}, \tilde{\rho}_{32}, \tilde{\rho}_{33})^T$ obeys the Liouville equation

$$\partial_\tau \tilde{\varrho}(\tau) = \mathcal{L} \tilde{\varrho}(\tau), \quad (\text{S16})$$

where \mathcal{L} is the Liouvillian super-operator expressed as 9×9 matrix, and formally evolves with time as $\tilde{\varrho}(\tau) = e^{\mathcal{L}\tau} \tilde{\varrho}(0)$. The vector $\tilde{\varrho}(\tau)$ is decomposed into $\tilde{\varrho}(n, \tau)$ which denotes the probability that n net photons have been emitted to the environment, such that $\tilde{\varrho}(\tau) = \sum_n \tilde{\varrho}(n, \tau)$. The $\tilde{\varrho}(n, \tau)$ satisfies the n -resolved master

equation [24]

$$\begin{aligned} \partial_\tau \tilde{\varrho}(n, \tau) &= \mathcal{L}_0 \tilde{\varrho}(n, \tau) \\ &+ \mathcal{L}_+ \tilde{\varrho}(n-1, \tau) + \mathcal{L}_- \tilde{\varrho}(n+1, \tau), \end{aligned} \quad (\text{S17})$$

where the generators \mathcal{L}_+ and \mathcal{L}_- are the off-diagonal element of the \mathcal{L} corresponding to the emissions ($\mathcal{L}_{22,11}, \mathcal{L}_{33,11}$) and absorption ($\mathcal{L}_{11,22}, \mathcal{L}_{11,33}$), respectively, and \mathcal{L}_0 is for the rest of the elements. Discrete Laplace transform $\hat{\varrho}_z(\tau) = \sum_n \hat{\varrho}(n, \tau) e^{zn}$, which satisfies $\lim_{z \rightarrow 0} \hat{\varrho}_z(\tau) = \varrho(\tau)$, casts Eq. (S17) into

$$\partial_\tau \hat{\varrho}_z(\tau) = \mathcal{L}(z) \hat{\varrho}_z(\tau) \quad (\text{S18})$$

with $\mathcal{L}(z) \equiv \mathcal{L}_0 + e^z \mathcal{L}_+ + e^{-z} \mathcal{L}_-$.

$$\mathcal{L}(z) \equiv \begin{bmatrix} -A_1 & -i\Omega_c & -i\Omega_p & i\Omega_c & \gamma \bar{n}_{12} e^{-z} & 0 & i\Omega_p & 0 & \bar{n}_{13} e^{-z} \\ -i\Omega_c & i\delta\omega_c - A_2 & 0 & 0 & i\Omega_c & 0 & 0 & i\Omega_p & 0 \\ -i\Omega_p & 0 & i\delta\omega_p - A_3 & 0 & 0 & i\Omega_c & 0 & 0 & i\Omega_p \\ i\Omega_c & 0 & 0 & -i\delta\omega_c - A_2 & -i\Omega_c & -i\Omega_p & 0 & 0 & 0 \\ \gamma(\bar{n}_{12} + 1)e^z & i\Omega_c & 0 & -i\Omega_c & -\gamma \bar{n}_{12} & 0 & 0 & 0 & 0 \\ 0 & 0 & i\Omega_c & -i\Omega_p & 0 & i\delta\omega_{pc} - A_6 & 0 & 0 & 0 \\ i\Omega_p & 0 & 0 & 0 & 0 & 0 & -i\delta\omega_p - A_3 & -i\Omega_c & -i\Omega_p \\ 0 & i\Omega_p & 0 & 0 & 0 & 0 & -i\Omega_c & -i\delta\omega_{pc} - A_6 & 0 \\ (\bar{n}_{13} + 1)e^z & 0 & i\Omega_p & 0 & 0 & 0 & -i\Omega_p & 0 & -\bar{n}_{13} \end{bmatrix}, \quad (\text{S19})$$

with $\delta\omega_{pc} = \delta\omega_p - \delta\omega_c$, $A_1 = \gamma(\bar{n}_{12} + 1) + (\bar{n}_{13} + 1)$, $A_2 = \gamma(2\bar{n}_{12} + 1)/2 - (\bar{n}_{13} + 1)/2$, $A_3 = \gamma(\bar{n}_{12} + 1)/2 - (2\bar{n}_{13} + 1)/2$, and $A_6 = (\gamma\bar{n}_{12} + \bar{n}_{13})/2$. Note that at $\tau \gg 1$, $\rho_z(\tau)$ is related with the largest eigenvalue $\lambda_0(z)$ of the modified super-operator $\mathcal{L}(z)$ as follows

$$\hat{\varrho}_z(\tau) = e^{\mathcal{L}(z)\tau} \hat{\varrho}_z(0) \sim e^{\lambda_0(z)\tau}. \quad (\text{S20})$$

Note that $\lambda_0(z)$ is obtained from the characteristic polynomial of $\mathcal{L}(z)$

$$\det |\lambda(z)\mathcal{I} - \mathcal{L}(z)| = \sum_{n=0}^9 a_n(z) \lambda^n(z) = 0. \quad (\text{S21})$$

The cumulant generating function $\mathcal{G}(z, \tau)$, defined by

$$\mathcal{G}(z, \tau) = \ln \langle e^{zn} \rangle = \ln \sum_n P(n, \tau) e^{zn}, \quad (\text{S22})$$

with $P(n, \tau) = \sum_{\alpha=1,2,3} \tilde{\rho}_{\alpha\alpha}(n, \tau)$ and $\sum_n P(n, \tau) = 1$, allows one to calculate the k -th cumulant

$$\langle \langle n^k \rangle \rangle(\tau) = \frac{\partial^k \mathcal{G}(z, \tau)}{\partial z^k} \Big|_{z=0}. \quad (\text{S23})$$

For $\tau \gg 1$, $\mathcal{G}(z, \tau) \sim \lambda_0(z)\tau$. Therefore, we obtain the

steady-state relation

$$\lim_{\tau \rightarrow \infty} \frac{\langle \langle n^k \rangle \rangle(\tau)}{\tau} = \frac{\partial^k \lambda_0(z)}{\partial z^k} \Big|_{z=0} \quad (\text{S24})$$

Eq.(S21) differentiated with respect to z at $z = 0$ yields $a'_0(0) + a_1(0)\lambda'_0(0) = 0$, and $a''_0(0) + a'_1(0)\lambda'_0(0) + a_1(0)\lambda''_0(0) + 2a_2(0)(\lambda'_0(0))^2 = 0$. Thus, the mean current and current fluctuations can be expressed in terms of the coefficients of the characteristic polynomial [30]

$$\begin{aligned} \langle j \rangle &= -\frac{a'_0(0)}{a_1(0)} \\ \text{var}[j] &= -\frac{[a''_0(0) + 2a'_1(0)\lambda'_0(0) + 2a_2(0)(\lambda'_0(0))^2]}{a_1(0)} \\ \mathcal{F} &= \frac{a''_0(0)}{a'_0(0)} \left[1 + \frac{2(a'_0(0))^2 a_2(0) - 2a'_0(0)a_1(0)a'_1(0)}{a''_0(0)(a_1(0))^2} \right]. \end{aligned} \quad (\text{S25})$$

Detailed calculations of coherences and Fano factor

The general expressions for the Fano factor and coherences at steady states are too lengthy to display; however, for the case of resonant control pulse ($\delta\omega_c = 0$) with $\mathcal{A} \gg 1$ (or $\bar{n} \sim 0$), the coherences and Fano factor at steady state are simplified and written in a manageable form.

$$\begin{aligned}
\tilde{\rho}_{11} &= \frac{4(\gamma+1)\Omega_c^2\Omega_p^2\delta\omega_p^2}{\mathcal{D}} \\
\tilde{\rho}_{22} &= \frac{\Omega_p^2 [\gamma \{(\gamma+1)^2 + 4\Omega_c^2\} \delta\omega_p^2 + 4(\Omega_c^2 + \Omega_p^2)(\Omega_c^2 + \gamma\Omega_p^2)]}{\mathcal{D}} \\
\tilde{\rho}_{33} &= \frac{\Omega_c^2 [4\delta\omega_p^4 + \{(\gamma+1)^2 - 8\Omega_c^2 + 4\Omega_p^2\} \delta\omega_p^2 + 4(\Omega_c^2 + \Omega_p^2)(\Omega_c^2 + \gamma\Omega_p^2)]}{\mathcal{D}} \\
\rho_{12}^R &= -\frac{4\Omega_c\Omega_p^2(\Omega_c^2 + \gamma\Omega_p^2)\delta\omega_p}{\mathcal{D}} \\
\rho_{12}^I &= \frac{2\gamma(\gamma+1)\Omega_c\Omega_p^2\delta\omega_p^2}{\mathcal{D}} \\
\rho_{13}^R &= \frac{4\Omega_c^2\Omega_p(\Omega_c^2 + \gamma\Omega_p^2 - \delta\omega_p^2)\delta\omega_p}{\mathcal{D}} \\
\rho_{13}^I &= \frac{2(\gamma+1)\Omega_c^2\Omega_p\delta\omega_p^2}{\mathcal{D}} \\
\rho_{23}^R &= \frac{4\Omega_c\Omega_p[\Omega_c^2\delta\omega_p^2 - (\Omega_c^2 + \Omega_p^2)(\Omega_c^2 + \gamma\Omega_p^2)]}{\mathcal{D}} \\
\rho_{23}^I &= -\frac{2(\gamma+1)(\Omega_c^2 + \gamma\Omega_p^2)\Omega_c\Omega_p\delta\omega_p}{\mathcal{D}}
\end{aligned} \tag{S26}$$

with $\mathcal{D} = 4\Omega_c^2\delta\omega_p^4 + [\gamma(\gamma+1)^2\Omega_p^2 + (\gamma+1)(\gamma+1+8\Omega_p^2)\Omega_c^2 - 8\Omega_c^4]\delta\omega_p^2 + 4(\Omega_c^2 + \Omega_p^2)^2(\Omega_c^2 + \gamma\Omega_p^2)$.

The coefficients of the characteristic polynomial of $\mathcal{L}(z)$ (Eq. (S21)) at $z = 0$, which are required for evaluating the quantities in Eq. (S25), are obtained as follows.

$$\begin{aligned}
a'_0(0) &= a''_0(0) = (\gamma+1)^3\Omega_c^2\Omega_p^2\delta\omega_p^2, \\
a_1(0) &= -(\gamma+1) \left[\Omega_c^2\delta\omega_p^4 + \{(\gamma+1)\Omega_c^2(\gamma+8\Omega_p^2+1) - 8\Omega_c^4 + \gamma(\gamma+1)^2\Omega_p^2\}(\delta\omega_p^2/4) + (\Omega_c^2 + \Omega_p^2)^2(\Omega_c^2 + \gamma\Omega_p^2) \right], \\
a'_1(0) &= (\gamma+1) \left[\gamma\Omega_c^2\delta\omega_p^4 + \{\gamma\Omega_c^2((\gamma+1)^2 - 8\Omega_c^2) + (\gamma+1)\Omega_p^2(20\Omega_c^2 + \gamma+1)\}(\delta\omega_p^2/4) + (\Omega_c^2 + \Omega_p^2)^2(\gamma\Omega_c^2 + \Omega_p^2) \right], \\
a_2(0) &= \frac{1}{16} \left[-4\{8(\gamma+2)\Omega_c^2 + (\gamma+1)^3\}\delta\omega_p^4 \right. \\
&\quad \left. + \{64(\gamma+2)\Omega_c^4 - 8\Omega_c^2(3(\gamma+1)^2 + 4(6\gamma+7)\Omega_p^2) - (\gamma+1)((\gamma+1)^4 + 8(4\gamma+1)(\gamma+1)\Omega_p^2 + 16\Omega_p^4)\}\delta\omega_p^2 \right. \\
&\quad \left. - 4(\Omega_c^2 + \Omega_p^2)\{8(\gamma+2)\Omega_c^4 + (\gamma+1)\Omega_c^2((\gamma+1)(\gamma+5) + 24\Omega_p^2) + 8(2\gamma+1)\Omega_p^4 + (\gamma+1)^2(5\gamma+1)\Omega_p^2\} \right].
\end{aligned} \tag{S27}$$

It can be shown that

$$\frac{2(a'_0(0))^2a_2(0) - 2a'_0(0)a_1(0)a'_1(0)}{a''_0(0)(a_1(0))^2} = 2 \sum_{i < j} (\tilde{\rho}_{ij}^R)^2 - 6 \sum_{i < j} (\tilde{\rho}_{ij}^I)^2 + q(\Omega_c, \Omega_p, \delta\omega_p, \gamma) \tag{S28}$$

where

$$q(\Omega_c, \Omega_p, \delta\omega_p, \gamma) = \frac{2q_n}{q_d} \tag{S29}$$

with

$$\begin{aligned}
q_n &= 16\gamma\Omega_c^4\delta\omega_p^8 - 8\gamma\Omega_c^2[8\Omega_c^4 - \{(\gamma+1)^2 + 2\Omega_p^2\}\Omega_c^2 + (\gamma+1)^2\Omega_p^2]\delta\omega_p^6 \\
&\quad + [96\gamma\Omega_c^8 - 16\gamma\Omega_c^6((\gamma+1)^2 - (\gamma+2)\Omega_p^2) + (\gamma+1)\Omega_c^4(\gamma(\gamma+1)^3 + 4\gamma(\gamma+1)\Omega_p^2 - 32\Omega_p^4) \\
&\quad - 2\gamma\Omega_c^2\Omega_p^2((\gamma+1)^4 + 6(\gamma+1)^2\Omega_p^2 + 16\Omega_p^4) + \gamma(\gamma+1)^4\Omega_p^4]\delta\omega_p^4 \\
&\quad - 4[16\gamma\Omega_c^{10} - 2\gamma\Omega_c^8\{(\gamma+1)^2 - 2(2\gamma+7)\Omega_p^2\} + \Omega_c^6\Omega_p^2\{\gamma(-\gamma^3 + 3\gamma + 2) + 4(3\gamma^2 + \gamma + 1)\Omega_p^2\} \\
&\quad + 2\Omega_c^4\Omega_p^4\{(\gamma^2 + \gamma + 1)(\gamma+1)^2 + 2((\gamma-3)\gamma + 1)\Omega_p^2\} + \Omega_c^2\Omega_p^6(\gamma(\gamma(2\gamma+3) - 4\Omega_p^2) - 1) - 2\gamma(\gamma+1)^2\Omega_p^8]\delta\omega_p^2 \\
&\quad + 16(\Omega_c^2 + \Omega_p^2)^2(\Omega_c^2 + \gamma\Omega_p^2)(\gamma\Omega_c^6 + 2\gamma\Omega_c^4\Omega_p^2 + 2\Omega_c^2\Omega_p^4 + \Omega_p^6) \\
q_d &= \left[4\Omega_c^2\delta\omega_p^4 - \{8\Omega_c^4 - (\gamma+1)(\gamma+1 + 8\Omega_p^2)\Omega_c^2 - \gamma(\gamma+1)^2\Omega_p^2\}\delta\omega_p^2 + 4(\Omega_c^2 + \Omega_p^2)^2(\Omega_c^2 + \gamma\Omega_p^2)\right]^2
\end{aligned}$$

For $\delta\omega_p = 0$,

$$\begin{aligned}
q(\cdot)|_{\delta\omega_p=0} &= \frac{32(\Omega_c^2 + \Omega_p^2)^2(\Omega_c^2 + \gamma\Omega_p^2)(\gamma\Omega_c^6 + 2\gamma\Omega_c^4\Omega_p^2 + 2\Omega_c^2\Omega_p^4 + \Omega_p^6)}{\left[4(\Omega_c^2 + \Omega_p^2)^2(\Omega_c^2 + \gamma\Omega_p^2)\right]^2} \\
&= \frac{2(\gamma\xi^6 + 2\gamma\xi^4 + 2\xi^2 + 1)}{(\xi^2 + 1)(\xi^2 + \gamma)^2}
\end{aligned} \tag{S30}$$

Whereas $q = 0$ in a coherently driven TLS [22], $q(\Omega_c, \Omega_p, \delta\omega_p, \gamma) \neq 0$ in the Λ -system contributes to the Fano factor of the transition current.

Although the expressions for $a_0(z)$ and $a_1(z)$ are lengthy and complicated, the total transition current $\langle j \rangle$ is straightforwardly decomposed into the two parts, $\langle j \rangle = \langle j \rangle_{12} + \langle j \rangle_{13}$ with

$$\langle j \rangle_{12} = \gamma(\bar{n}_{12} + 1)\tilde{\rho}_{11}^{ss} - \gamma\bar{n}_{12}\tilde{\rho}_{22}^{ss} = 2\Omega_c\tilde{\rho}_{12}^I \tag{S31}$$

and

$$\langle j \rangle_{13} = (\bar{n}_{13} + 1)\tilde{\rho}_{11}^{ss} - \bar{n}_{13}\tilde{\rho}_{33}^{ss} = 2\Omega_p\tilde{\rho}_{13}^I. \tag{S32}$$

The first equalities of Eqs. S31 and S32 are consistent with the definition of reaction current between two discrete states in classical Markov jump system, and this can also be related with the imaginary part of coherence between the two quantum states, which is called *current-coherence* relation [31].

Relation between v_g and \mathcal{F}

For the case of resonant control pulse ($\delta\omega_c = 0$) with $\mathcal{A} \gg 1$ (or $\bar{n} \sim 0$), when $(\partial\rho_{13}^R/\partial\omega_p)_{\delta\omega_p=0} = \Omega_p^{-1}\xi^2/(\xi^2 + 1)^2$ is inserted to Eq. (6), we get an expression of the group velocity in terms of ξ .

$$v_g = \frac{c}{1 + \frac{\mathcal{N}\xi^2}{(\xi^2 + 1)^2}} \tag{S33}$$

with $\mathcal{N} \equiv 2\pi N_d\omega_p/\Omega_p$.

For the two-photon resonance ($\delta\omega_c = \delta\omega_p = 0$), the Fano factor is contributed only by the real part of coherence between $|2\rangle$ and $|3\rangle$ ($\rho_{23}^R \neq 0$) while others vanish ($\rho_{12}^R = \rho_{12}^I = \rho_{13}^R = \rho_{13}^I = \rho_{23}^I = 0$), which simplifies \mathcal{F} into

$$\mathcal{F} = 1 + 2(\rho_{23}^R)^2 \Big|_{\delta\omega_p=0} + q(\xi, \gamma) \tag{S34}$$

with

$$\begin{aligned}
(\rho_{23}^R)^2 \Big|_{\delta\omega_p=0} &= \frac{\xi^2}{(\xi^2 + 1)^2} \\
q(\xi, \gamma) \Big|_{\delta\omega_p=0} &= \frac{2(\xi^6\gamma + 2\xi^4\gamma + 2\xi^2 + 1)}{(\xi^2 + 1)^2(\xi^2 + \gamma)}.
\end{aligned} \tag{S35}$$

Insertion of Eq. (S35) into Eq. (S34) yields Eq. (8).

Laser power and Rabi frequency

For a plane wave the average intensity can be expressed as

$$\langle I_\alpha \rangle = \frac{c}{8\pi}\zeta_\alpha^2 \quad \alpha \in c, p. \tag{S36}$$

Now by considering the polarization of incident light parallel to the dipole, we can write $\zeta_\alpha = \hbar\Omega_\alpha/|d_{ij}|$ which yields

$$\langle I_\alpha \rangle = \frac{c\hbar^2\Omega_\alpha^2}{8\pi|d_{ij}|^2}, \tag{S37}$$

and from the spontaneous decay we know $(\hbar/|d_{ij}|)^2 = 16\pi^2 h/3\gamma_{ij}\lambda_\alpha^3$. Thus, we obtain the relationship between the average intensity of the laser pulse ($\langle I_\alpha \rangle$),

reported in the literatures [1], and other quantities,

$$\langle I_\alpha \rangle = \frac{2\pi hc\Omega_\alpha^2}{3\gamma_{ij}\lambda_\alpha^3}. \quad (\text{S38})$$